Energy-based theory of autoresonance in chains of coupled damped-driven generic oscillators

Ricardo Chacón[1], Faustino Palmero[2], Pedro J. Martínez[3], and Somnath Roy[4]
[1]*Departamento de Física Aplicada, E.I.I., Universidad de Extremadura, Apartado Postal 382, E-06006 Badajoz, Spain and Instituto de Computación Científica Avanzada (ICCAEx), Universidad de Extremadura, E-06006 Badajoz, Spain*
[2]*Grupo de Física No Lineal, Departamento de Física Aplicada I, Escuela Técnica Superior de Ingeniería Informática, Universidad de Sevilla, Avda Reina Mercedes s/n, E-41012 Sevilla, Spain*
[3]*Departamento de Física Aplicada, E.I.N.A., Universidad de Zaragoza, E-50018 Zaragoza, Spain and Instituto de Nanociencia y Materiales de Aragón (INMA), CSIC-Universidad de Zaragoza, E-50009 Zaragoza, Spain and*
[4]*Department of Applied Mechanics, Indian Institute of Technology Madras, Chennai, Tamil Nadu 600036, India*
(Dated: July 23, 2024)

An energy-based theory of autoresonance in driven dissipative chains of coupled generic oscillators is discussed on the basis of a variational principle concerning the energy functional. The theory is applied to chains of delayed Duffing-Ueda oscillators and the equations that together govern the autoresonance forces and solutions are derived and solved analytically for generic values of parameters and initial conditions, including the case of quenched time-delay disorder. Remarkably, the presence of retarded potentials with time-delayed feedback drastically modify the autoresonance scenario preventing the growth of the energy oscillation over specific regions of the parameter space. Additionally, effective harmonic forces with a slowly varying frequency are derived from the exact autoresonant excitations and the effectiveness of the theory is demonstrated at suppressing the chaos induced by homogeneous periodic excitations in such oscillator chains. Numerical experiments confirmed all the theoretical predictions.

PACS numbers: 05.45. -a

I. INTRODUCTION

Autoresonance (AR) induced secular growth of the oscillation energy in nonlinear damped-driven systems take place when the system persistently adjusts its amplitude so that its instantaneous nonlinear period balances the driving period. Firstly studied in Hamiltonian systems, AR phenomena have been investigated since the middle of the last century and have been noted in diverse contexts: particle accelerators [1, 2], atomic and molecular physics [3], planetary dynamics [4], nonlinear low-dimensional oscillators [5], nanoscale magnetic devices [6], nonlinear chains subject to localized driving [7], plasma waves [8], and energy transfer between axions [9], to quote a few instances. While most previous investigations on AR have restricted themselves to explore the effectiveness of chirped harmonic forces [1–10], a general energy-based AR (EBAR) theory has been proposed to explain the approximate and phenomenological findings arising from a prior adiabatic approach to AR in Duffing-like oscillators [11]. Further application of the EBAR theory to low-dimensional systems has included the case where the system crosses a separatrix associated with its underlying integrable counterpart [12] as well as the problem of chaotic escape in dissipative multistable systems [13]. Since the application of chirped harmonic forces to give rise to reliable autoresonant responses in multi-particle chains seems to be more problematic than in the case of an isolated oscillator [14], the question naturally arises: How does an extension of the EBAR theory to driven dissipative chains of coupled generic oscillators work?

The remainder of the communication is organized as follows. In Sec. II, we provide the extension of the EBAR theory to driven dissipative chains of coupled generic oscillators. Section III applies the theory developed in Sec. II to chains of Duffing-Ueda oscillators with time-delayed feedback and the equations that together govern the AR forces and solutions are derived and solved analytically for generic values of parameters and initial conditions. The effects of quenched time-delay disorder are discussed in Sec. IV, while Sec. V is devoted to an exploration of the effectiveness of the theory at controlling the chaos induced by homogeneous periodic excitations in Duffing-Ueda oscillator chains. Finally, we conclude with Sec. VI by summarizing our conclusions and discussing future extensions and applications of the EBAR theory. Some analytical calculations and numerical results are relegated to the Appendixes.

II. THEORY

The present extension of the EBAR theory is studied in the context of the family of N linearly coupled, identical oscillators

$$\ddot{u}_n + V'(u_n) = -\eta\dot{u}_n + \lambda\Delta_d u_n + F_n(t), \qquad (1)$$

where dots indicate time derivative, $\Delta_d u_n \equiv u_{n+1} + u_{n-1} - 2u_n$ is the discrete Laplacian operator, $V'(u_n) \equiv dV/du_n$ with $V(u_n)$ being a general on-site potential, η and λ are the damping coefficient and coupling constant, respectively, while $F_n(t)$ is a temporal force. Clearly, the corresponding equation for the energy is

$$\begin{aligned}\dot{E} &= \sum_n \dot{u}_n \left[-\eta \dot{u}_n + F_n(t) + \lambda \Delta_d u_n\right] \\ &+ \lambda \sum_n \left(\dot{u}_{n+1} - \dot{u}_n\right)\left(u_{n+1} - u_n\right) \\ &\equiv P\left(u_1, ..., u_N, \dot{u}_1, ..., \dot{u}_N, t\right), \end{aligned} \tag{2}$$

where

$$E \equiv \sum_n \left[\dot{u}_n^2/2 + V\left(u_n\right)\right] + \frac{\lambda}{2}\sum_n \left(u_{n+1} - u_n\right)^2 \tag{3}$$

and $P\left(u_1, ..., u_N, \dot{u}_1, ..., \dot{u}_N, t\right)$ are the energy and power, respectively. As in the case of isolated oscillators, the AR solutions of Eq. (1) are defined in terms of a variational principle by imposing that the energy variation $\Delta E = \int_{t_1}^{t_2} P\left(u_1, ..., u_N, \dot{u}_1, ..., \dot{u}_N, t\right) dt$ is a maximum (with t_1, t_2 arbitrary but fixed instants) under the influence of dissipation and forcing. Thus, the corresponding Euler-Lagrange equations provide the necessary conditions (AR conditions) to be fulfilled by the AR solutions and temporal forces:

$$\frac{\partial P}{\partial u_n} - \frac{d}{dt}\left(\frac{\partial P}{\partial \dot{u}_n}\right) = 0, \tag{4}$$

$n = 1, ..., N$. Indeed, Eq. (4) supply relationships between u_n, $\dot{u}_n$, and F_n such that the solutions of the system given by Eqs. (1) and (4) together provide the AR forces, $F_{n,AR}(t)$, and the AR solutions, $u_{n,AR}(t)$, for each set of initial conditions:

$$\ddot{u}_{n,AR} + V'(u_{n,AR}) = \eta \dot{u}_{n,AR} + \lambda \Delta_d u_{n,AR}, \tag{5}$$

$$F_{n,AR}(t) = 2\eta \dot{u}_{n,AR}, \tag{6}$$

$n = 1, ..., N$. Clearly, this AR scenario is strongly dependent upon the distribution of initial conditions: while for non-uniform distributions the AR forces and solutions depend upon the coupling constant through the discrete Laplacian operator, for uniform distributions the coupling energy is always zero (a situation equivalent to that of the anticontinous limit $\lambda = 0$), and hence the AR forces and solutions are those corresponding to the respective isolated oscillators. Regarding the Hamiltonian limiting case $\eta \to 0$, notice that Eq. (5) can be equivalently rewritten as

$$\ddot{u}_{n,AR} + V'(u_{n,AR}) = F_{n,AR}/2 + \lambda \Delta_d u_{n,AR} \tag{7}$$

[cf. Eq. (6)], which suggests the natural ansatz [11] $F_{n,AR}(t) = \kappa \dot{u}_{n,AR}, \kappa > 0$, for Hamiltonian chains ($\eta = 0$) and where the AR rate, κ, is a free parameter controlling the initial force strength. Therefore, one can expect that the AR solutions and forces for the Hamiltonian case are essentially the same than those for the dissipative case, both with κ instead of η.

III. DUFFING-UEDA OSCILLATORS WITH TIME-DELAYED FEEDBACK

Let us consider the application of the above EBAR theory to the significant instance of purely nonlinear (cubic) oscillators with a homogeneous retarded potential with time-delayed feedback $V'(u_n) = \beta u_n^3 + \alpha u_n\left(t - \tau\right)$ [cf. Eq. (1)], with the positive parameters α and τ accounting for the strength and time-delay of the retardation term, respectively. Time delays are unavoidable in real-world systems since they are induced because of the finite time needed to exchange information in complex (coupled) systems [15]. After assuming that τ is sufficiently small such that

$$u_n\left(t - \tau\right) = u_n(t) - \tau \dot{u}_n\left(t\right) + \tau^2 \ddot{u}_n\left(t\right)/2 + O\left(\tau^3\right), \tag{8}$$

Eqs. (5) and (6) become

$$\ddot{u}_{n,AR} + \omega_0^2 u_{n,AR} + B u_{n,AR}^3 = \delta \dot{u}_{n,AR} + \Lambda \Delta_d u_{n,AR}, \tag{9}$$

$$F_{n,AR}(t) = 2\delta R \dot{u}_{n,AR}, \tag{10}$$

$n = 1, ..., N$, with $\omega_0^2 \equiv \alpha/R, R \equiv 1 + \alpha\tau^2/2, B \equiv \beta/R, \delta \equiv \left(\eta - \alpha\tau\right)/R, \Lambda \equiv \lambda/R$. Thus, when N is a multiple of 4 [16] and periodic boundary conditions are assumed, Eqs. (9) and (10) present AR solutions and forces

$$u_{n,AR}(t) = \gamma_0 \, \mathrm{e}^{\delta t/3} \, \mathrm{cn}\left[\varphi_n\left(t\right); \frac{1}{2}\right], \tag{11}$$

$$\begin{aligned} F_{n,AR}(t) &= \frac{2}{3}\gamma_0 \delta^2 R \, \mathrm{e}^{\delta t/3} \, \mathrm{cn}\left[\varphi_n\left(t\right); \frac{1}{2}\right] \\ &- 2\gamma_0^2 \delta R \sqrt{B} \, \mathrm{e}^{2\delta t/3} \, \mathrm{sn}\left[\varphi_n\left(t\right); \frac{1}{2}\right] \mathrm{dn}\left[\varphi_n\left(t\right); \frac{1}{2}\right], \end{aligned} \tag{12}$$

with the constraint $\Lambda = \delta^2/9 - \omega_0^2/2$, i.e.,

$$\left(1 + \frac{\alpha\tau^2}{2}\right)(\alpha + 2\lambda) = \frac{2}{9}(\eta - \alpha\tau)^2 \tag{13}$$

(see Fig (1)), and where cn, sn, dn are Jacobian elliptic functions of parameter m,

$$\varphi_n\left(t\right) \equiv 3\gamma_0 \delta^{-1} B^{1/2} \, \mathrm{e}^{\delta t/3} + n \, \mathrm{K}(1/2) + \phi_0, \tag{14}$$

with γ_0, ϕ_0 being arbitrary constants and $\mathrm{K}(m)$ the complete elliptic integral of the first kind, while the initial conditions satisfy the relationships

$$\begin{aligned} u_{n,AR}(0) &= \gamma_0 \, \mathrm{cn}\left[\varphi_n\left(0\right); \frac{1}{2}\right], \\ \dot{u}_{n,AR}(0) &= \frac{1}{3}\gamma_0 \delta R \, \mathrm{cn}\left[\varphi_n\left(0\right); \frac{1}{2}\right] - \gamma_0^2 \sqrt{B} \, \mathrm{sn}\left[\varphi_n\left(0\right); \frac{1}{2}\right] \\ &\mathrm{dn}\left[\varphi_n\left(0\right); \frac{1}{2}\right]. \end{aligned} \tag{15}$$

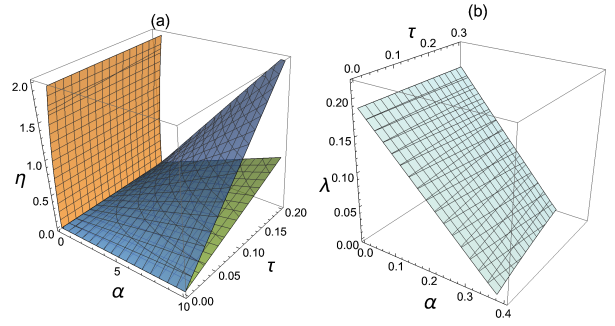

FIG. 1: (a) Constrain condition for $\lambda = 0$ [Eq. (13)] (leftmost surface), critical damping $\eta = \eta_c$ [cf. Eq. (16)], and critical damping $\eta = \eta_{c,mf}$ [cf. Eq. (29)] (rightmost surface). (b) Constrain condition for $\eta = 1.3$ [Eq. (13)].

In the two cases of homogeneous initial conditions and anticontinous limit, the system [Eq. (9)] reduces to a set of uncoupled oscillators and the corresponding general AR solutions and forces are those given by Eqs. (11) and (12) with $\varphi_n(t) \equiv 3\gamma_0\ \delta^{-1}B^{1/2}\,\mathrm{e}^{\delta t/3} + \phi_0$ for any N and arbitrary boundary conditions, while the constraint reduces to $\omega_0^2 = 2\delta^2/9$ [11]. Mathematically, the constraint is precisely the same condition for Eq. (9) to present, in the anticontinous limit, both the Painlevé property and a nontrivial Lie symmetry [17], indicating thus that such an equation is integrable. Remarkably, there exists a *critical* value of the damping coefficient,

$$\eta = \eta_c \equiv \alpha\tau, \tag{16}$$

such that for $\eta > \eta_c$ one has genuine AR solutions and forces given by Eqs. (11) and (12), while for $\eta < \eta_c$ the Euler-Lagrange equations [Eq. (4)] provide a necessary condition for the energy functional to present a minimum (i.e., that energy corresponding to equilibria). Physically, the constrain establishes a necessary condition to be satisfied by the strengths of dissipation, coupling, and retardation parameters for the energy amplification (decrease) rate to be maximum when $\eta > \eta_c$ ($\eta < \eta_c$). Furthermore, Eq. (9) can be derived from a Lagrangian

$$\mathcal{L} = \frac{\mathrm{e}^{-\delta t}}{2}\sum_n \left[\dot{u}_n^2 - \omega_0^2 u_n^2 - \frac{B u_n^4}{2} - \Lambda(u_{n+1}-u_n)^2\right], \tag{17}$$

whose associated Hamiltonian is

$$H = \sum_n \left\{\frac{\mathrm{e}^{\delta t}\,p_n^2}{2} + \frac{\mathrm{e}^{-\delta t}}{2}\left[\omega_0^2 u_n^2 + \frac{B u_n^4}{2} + \Lambda(u_{n+1}-u_n)^2\right]\right\}, \tag{18}$$

where $p_n \equiv \partial\mathcal{L}/\partial\dot{u}_n = \mathrm{e}^{-\delta t}\,\dot{u}_n$. For the critical damping $\eta = \eta_c$, the Hamiltonian is time-independent and energy is thereby conserved. After using the canonical transformation $U_n = u_n\,\mathrm{e}^{-\delta t/2}, P_n = p_n\,\mathrm{e}^{\delta t/2}$, together with the generating function $F_2 = \sum_n u_n P_n\,\mathrm{e}^{-\delta t/2}$ [18], the new Hamiltonian reads

$$K = \frac{1}{2}\sum_n \left[P_n^2 + \omega_0^2 U_n^2 + \frac{B}{2}\,\mathrm{e}^{\delta t}\,U_n^4\right] + \frac{1}{2}\sum_n \left[\Lambda(U_{n+1}-U_n)^2 - \delta P_n U_n\right], \tag{19}$$

and one obtains (after expanding $\mathrm{e}^{\delta t}$) that the AR solutions are associated (in terms of the old canonical variables and parameters) with the *adiabatic* invariant

$$\sum_n \left(\frac{p_n^2}{2} + \frac{\alpha u_n^2}{2+\alpha\tau^2} + \frac{\beta u_n^4}{4+2\alpha\tau^2}\right) + \sum_n \left[\frac{\lambda(u_{n+1}-u_n)^2 - (\eta-\alpha\tau)\,p_n u_n}{2+\alpha\tau^2}\right] \tag{20}$$

over the time interval $0 \leqslant t \lesssim t_{AI}$,

$$t_{AI} \sim \delta^{-1} \sim \left[\left(1+\alpha\tau^2/2\right)/\left(\lambda+\alpha/2\right)\right]^{1/2} \tag{21}$$

[cf. Eq. (13)], with t_{AI} being the onset time for AR. Thus, t_{AI} provides a time scale from which the energy amplification effects are noticeable when $\eta > \eta_c$. When $\eta \to \eta_c$, Eq. (13) cannot be satisfied, while $t_{AI} \to \infty$ and hence Eq. (20) provides the aforementioned invariant (energy) due to $F_{n,AR}(t) \to 0$ [cf. Eq. (12)]. When $\lambda \to 0$, the adiabatic invariant Eq. (20) reduces to a set of N identical adiabatic invariants corresponding to a set of N uncoupled Duffing-Ueda oscillators. Extensive numerical simulations confirmed all the features of the present AR scenario [see Fig. (2)].

Next, we derive effective chirped harmonic forces from Eq. (12) for $\eta > \eta_c$. For $t \lesssim t_b$,

$$t_b \sim \delta^{-1} \sim \left[\left(1+\alpha\tau^2/2\right)/\left(\lambda+\alpha/2\right)\right]^{1/2} \tag{22}$$

[cf. Eq. (13)], with t_b being the breaking time for AR [5], and, e.g., homogeneous initial conditions near equilibria ($u_i(0) \simeq 0, \dot{u}_i(0) \simeq 0, i = 1, ..., N$), one straightforwardly obtains

$$F_{n,AR}(t) \simeq \frac{2}{3}\gamma_0\,(\eta-\eta_c)^2\cos\left[\Omega(t)\,t\right], \tag{23}$$

$$\Omega(t) \equiv \frac{3\gamma_0\sqrt{2\alpha\beta}}{2\,(\eta-\eta_c)}\left[1 + \frac{3\alpha}{4\,(\eta-\eta_c)}t\right] \tag{24}$$

which is of the form $\varepsilon\cos\left(\Omega_0 t + \xi t^2/2\right)$ [5], with ε and ξ being the amplitude and linear sweep rate, respectively. Therefore, the EBAR theory predicts the following scale laws for the respective thresholds for AR:

$$\varepsilon_{th} \sim (\eta-\alpha\tau)^2\,,\ \xi_{th} \sim \alpha^{3/2}\,(\eta-\alpha\tau)^{-2}\,. \tag{25}$$

Notice that chirped harmonic forces valid for arbitrary initial conditions can be straightforwardly calculated from Eq. (12) (see Appendix A for an explicit expression).

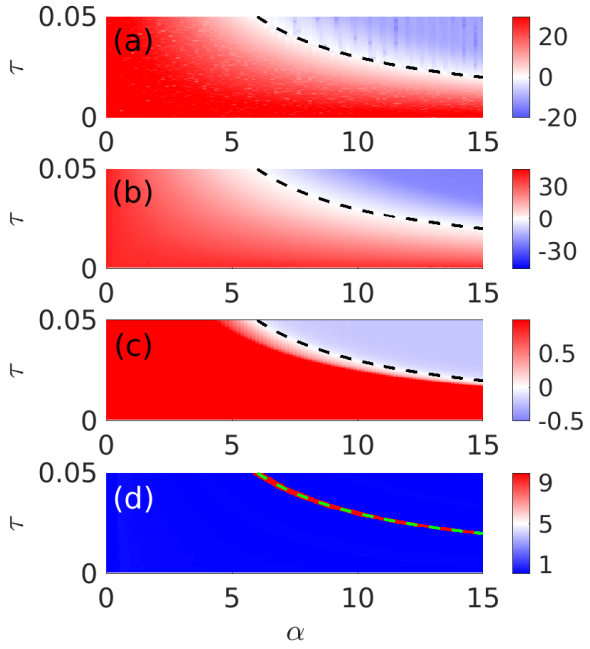

FIG. 2: (a), (b), (c) Energy amplification, $\log\left[E\left(t=t_{\max}\right)/E\left(t=0\right)\right]$, in the $\alpha-\tau$ parameter plane for a ring of $N=15$ oscillators with $\beta=1, \eta=0.3$ and $t_{\max}=100$. (a) Isolated oscillator ($\lambda=0$). (b) Case where the exact AR force is applied to all oscillators and $\lambda=0.1$. (c) Case where the exact AR force is applied to a single oscillator and $\lambda=0.1$. (d) Dimensionless onset time for AR (δt), after which the adiabatic invariant [Eq. (20)] undergoes a deviation equal to 10% with respect to its initial value. The initial conditions are randomly and independently chosen. The dashed lines (green (grey) in version (d)) indicate the critical damping $\eta=\eta_c$ [cf. Eq. (16)] separating the amplification regime from the extinction regime.

IV. TIME-DELAY DISORDER

We study the effects of quenched disorder on the above AR scenario by randomly choosing the time-delays τ_n uniformly from the interval $[0,\tau_{\max}]$. Thus, Eqs. (9) and (10) become a family of randomly AR equations (one for each sampling of the uniform distribution) with $\omega_0^2, B, \delta, \Lambda$ being disorder-induced random parameters having averages

$$\begin{aligned}
\left\langle\omega_0^2\right\rangle &= \tau_{\max}^{-1}\alpha\sqrt{2/\alpha}\arctan\left(\sqrt{\alpha/2}\tau_{\max}\right),\\
\left\langle B\right\rangle &= \tau_{\max}^{-1}\beta\sqrt{2/\beta}\arctan\left(\sqrt{\beta/2}\tau_{\max}\right),\\
\left\langle \Lambda\right\rangle &= \tau_{\max}^{-1}\lambda\sqrt{2/\lambda}\arctan\left(\sqrt{\lambda/2}\tau_{\max}\right),\\
\left\langle \delta\right\rangle &= \tau_{\max}^{-1}\eta\sqrt{2/\alpha}\arctan\left(\sqrt{\alpha/2}\tau_{\max}\right)\\
&\quad-\tau_{\max}^{-1}\ln\left(1+\alpha\tau_{\max}^2/2\right),
\end{aligned} \tag{26}$$

and where $\langle\cdot\rangle\equiv\tau_{\max}^{-1}\int_0^{\tau_{\max}}(\cdot)\,d\tau_n$. Therefore, the effective (mean-field) AR equations reads

$$\begin{aligned}
\ddot{u}_{n,AR}+\left\langle\omega_0^2\right\rangle u_{n,AR}+\left\langle B\right\rangle u_{n,AR}^3 &= \left\langle\delta\right\rangle\dot{u}_{n,AR} \\
&\quad+\left\langle\Lambda\right\rangle\Delta_d u_{n,AR}, \qquad (27)\\
\left\langle 1/R\right\rangle F_{n,AR}(t) &= 2\left\langle\delta\right\rangle\dot{u}_{n,AR}, \qquad (28)
\end{aligned}$$

whose solutions are given by Eqs. (11) and (12) with obvious substitutions. Remarkably, this mean-field approach also predicts the existence of a critical value of the damping coefficient,

$$\eta=\eta_{c,mf}\equiv\frac{\sqrt{\alpha/2}\ln\left(1+\alpha\tau_{\max}^2/2\right)}{\arctan\left(\sqrt{\alpha/2}\tau_{\max}\right)}, \tag{29}$$

such that for $\eta>\eta_{c,mf}$ one has optimal energy amplification on average, while for $\eta<\eta_{c,mf}$ the chain's energy tends to a minimum on average, which indicates the *robustness* of the above AR scenario against the presence of quenched time-delay disorder. Note that $\eta_{c,mf}\to\eta_c$ with $\tau=\tau_{\max}/2$ when $\tau_{\max}\to 0$, as expected [cf Fig. 1(a)]. We found that quenched time-delay disorder favors the energy's amplification with respect to the homogeneous case, as predicted from the above mean field approximation and is confirmed by numerical experiments (see Fig. 3).

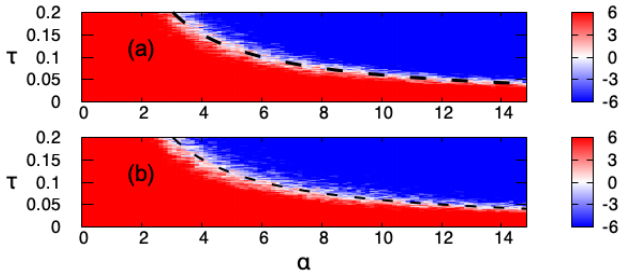

FIG. 3: Energy amplification, $\log\left[E\left(t=t_{\max}\right)/E\left(t=0\right)\right]$, in the $\alpha-\tau_{\max}$ parameter plane for $\beta=1, \eta=0.3, t_{\max}=50$. (a) Isolated oscillator ($\lambda=0$). (b) Ring of $N=5$ oscillators with $\lambda=0.1$ and where the retardation term and the exact AR force are solely applied to a single oscillator, while the initial conditions are randomly and independently chosen. The dashed lines indicate the critical damping $\eta=\eta_{c,mf}$ [cf. Eq. (29)] separating the amplification regime from the extinction regime.

V. AR-INDUCED CHAOS SUPPRESSION

Since local injection and absorption of energy can modify a chain´s energy landscapes, and hence reshape the basins of attraction of the possible attractors in phase space, we study the effectiveness of retardation terms and AR forces at suppressing the chaos arising from Duffing-Ueda chains when the oscillators are solely subjected to

dissipation and homogeneous harmonic driving:

$$\ddot{u}_n + \beta u_n^3 = -\eta \dot{u}_n + \gamma \cos(\omega t) + \lambda \Delta_d u_n, \tag{30}$$

$n = 1, ..., N$. Thus, for the case $V'(u_n) = \beta u_n^3 + \alpha u_n(t-\tau) - \gamma \cos(\omega t)$ [cf. Eq. (1)], Eqs. (5) and (6) become

$$\ddot{u}_{n,AR} + \omega_0^2 u_{n,AR} + B u_{n,AR}^3 = \delta \dot{u}_{n,AR} + \Lambda \Delta_d u_{n,AR}, \tag{31}$$

$$F_{n,AR}(t) = 2\delta R \dot{u}_{n,AR} - \gamma \cos(\omega t) \tag{32}$$

$n = 1, ..., N$. Clearly, the AR solutions are the same for the cases with and without homogeneous periodic driving, but the corresponding AR forces differ precisely in such a periodic force [cf. Eqs. (10) and (32)]. Now, we explore the effectiveness of locally applying AR forces on M $(1 \leqslant M \leqslant N)$ oscillators at suppressing the chaos existing for $\alpha = F_n(t) = 0$. Two suppressory scenarios are expected depending on whether η is greater or less than η_c. When $\eta > \eta_c$, one has an optimal local injection of energy on each of the M oscillators subjected to AR forces. Since these M oscillators act as energy sources for the remaining oscillators, after a certain time interval $\Delta t = t_f - t_i$, with t_i and t_f being the initial and final instants for the application of the AR forces, and also depending upon the remaining parameters, the chain's energy E is expected to reach a sufficiently high value to allow the chain to escape from the basin of the chaotic attractor (scenario I). However, this scenario is solely expected to be fully effective in the presence of multistability, i.e., when the damping coefficient is sufficiently small to allow the coexistence of a number of attractors for a fixed set of parameters. On the contrary, one has a monotonous loss of energy in each of the M oscillators when $\eta < \eta_c$, i.e., they are behaving as energy sinks for the chain's energy. This loss of energy may again, depending upon the remaining parameters, allow the chain to escape from the basin of the chaotic attractor, thus regularizing its dynamics (scenario II). While the former scenario seems less effective and less far-reaching than the latter scenario, Fig. 4 shows illustrative examples confirming these two regularization scenarios. Typically, we found that regularized states are period-1 solutions of different waveforms, the regularization-inducing desynchronization of the chain when $M \ll N$ being maximum in the weak coupling regime and appearing due to cluster synchronization of different sets of oscillators (see Appendix B for further numerical details).

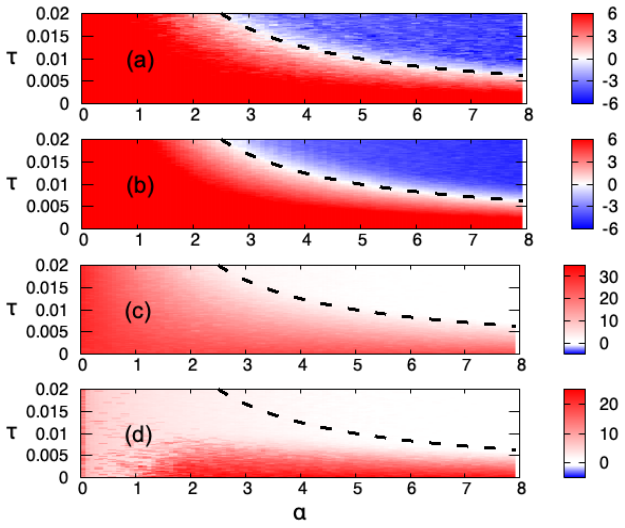

FIG. 4: (a), (b) Energy amplification, $\log[E(t = t_{\max})/E(t = 0)]$, in the $\alpha - \tau$ parameter plane for a ring of $N = 5$ oscillators with $t_{\max} = 200$. (a) Isolated oscillator ($\lambda = 0$). (b) Case where the retardation term and the exact AR force are applied to all oscillators and $\lambda = 0.1$. (c), (d) Average energy amplification, $\log[\langle E\rangle / \langle E_0\rangle]$ with $\langle E\rangle \equiv (4\pi/\omega)^{-1} \int_{t_{\max}-4\pi/\omega}^{t_{\max}} E(t)dt$, $\langle E_0\rangle \equiv (4\pi/\omega)^{-1} \int_{t_0}^{t_0+4\pi/\omega} E(t)dt$, in the $\alpha - \tau$ parameter plane for a ring of $N = 5$ oscillators with $t_0 = 40, t_{\max} = 400$, and where the retardation term and the exact AR force are solely applied to a single oscillator. (c) $\lambda = 0.01$. (d) $\lambda = 0.05$. The dashed lines indicate the critical damping $\eta = \eta_c$ [cf. Eq. (16)] separating the amplification regime from the extinction (regularization) regime (blank region). The chains present a chaotic attractor for $\alpha = F_n(t) = 0$. Fixed parameters: $\beta = 1, \eta = 0.05, \gamma = 0.1, \omega = 0.21$.

VI. CONCLUSION

We have developed a general energy-based theory of AR in damped driven chains of coupled generic oscillators and applied it to chains of delayed Duffing-Ueda oscillators to reveal a quite complex scenario of AR. This scenario provides accurate indications on how locally and optimally control the injection and absorption of energy to modify the global dynamics of the oscillator chains, in particular, of the order↔chaos transitions, including the case of quenched time-delay disorder. In contrast to previous approaches to AR in oscillator chains [7], in which chirped harmonic forces are systematically used, the present theory provides exact AR solutions and forces, from which useful chirped harmonic forces are derived and the limits of their effectiveness in parameter space are established. Future developments and applications of the present theory involve the control of topological solitons in Frenkel-Kontorova lattices as well as the control of dynamics in complex networks of damped-driven nonlinear systems.

Acknowledgments

Financial support from the Ministerio de Ciencia, Innovación y Universidades (MICIU, Spain) through Project No. PID2019-108508GB-I00/AEI/10.13039/501100011033 cofinanced by FEDER

funds (R.C., F.P.) is gratefully acknowledged. P.J.M. acknowledges support from Departamento de Industria e Innovación del Gobierno de Aragón (FENOL group, Grant No. E36-23R) and from the Ministerio de Ciencia, Innovación y Universidades (MICIU, Spain) through Project No. PID2020-113582GB-I00/AEI/10.13039/501100011033.

VII. APPENDIX A: CHIRPED HARMONIC FORCES FOR ARBITRARY INITIAL CONDITIONS

From the expression for the exact AR forces [cf. Eq. (12)], and for arbitrary initial conditions $\left(u_n(0), \dot{u}_n(0)\right)$, one straightforwardly obtains the generic harmonic approximation

$$F_{n,AR}(t) \approx 3\gamma_0(\alpha+2\lambda)k_1 \cos[\Omega'(t)t + n\pi/2] - 3\gamma_0^2 k_2 \left\{1 + \frac{2\cos\left[2\Omega'(t)t + n\pi\right]}{\cosh \pi}\right\} \sqrt{2\beta(\alpha+2\gamma)} \sin\left[\Omega'(t)t + n\pi/2\right], \tag{A1}$$

$$\Omega'(t) \equiv \frac{3\gamma_0 k_3 \sqrt{2\beta\,(\alpha+2\lambda)}}{2\,(\eta-\eta_c)} \left[1 + \frac{3\,(\alpha+2\lambda)}{4\,(\eta-\eta_c)} t\right], \tag{A2}$$

where $k_1 \equiv \pi\sqrt{2}/\left[K(1/2)\cosh(\pi/2)\right] \approx 0.95, k_2 \equiv \pi^2\sqrt{2}/\left[2K^2(1/2)\sinh(\pi/2)\right] \approx 0.88, k_3 \equiv \pi/\left[2K(1/2)\right] \approx 0.93$. Figure 5 shows a comparison between the exact [Eq. (12)] and the approximate [Eq. (A1)] autoresonance forces for a ring of $N = 16$ oscillators. Notice that the pattern shown for four correlative oscillators is repeated along the ring for the following oscillators.

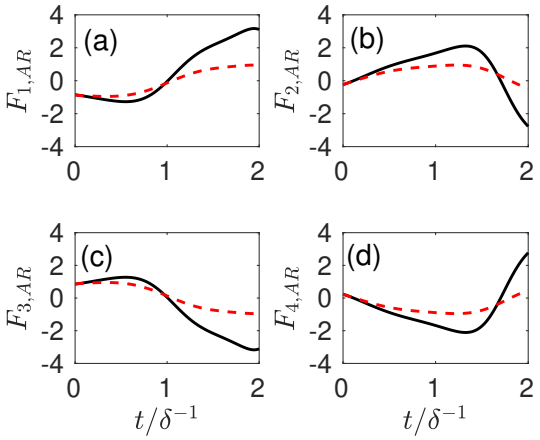

FIG. 5: Exact [Eq. (12), solid lines] and approximate [Eq. (A1), dashed lines] autoresonance excitations for a ring of $N = 16$ oscillators. (a) $n = 1$. (b) $n = 2$. (c) $n = 3$. (d) $n = 4$. Fixed parameters: $\beta = 1, \eta = 0.6, \alpha = 0.05, \tau = 0.01, \lambda = 0.015$.

VIII. APPENDIX B: ADDITIONAL NUMERICAL RESULTS

Figure 6 shows the average energy amplification, $\log\left[\langle E\rangle / \langle E_0\rangle\right]$, where

$$\langle E\rangle \equiv (4\pi/\omega)^{-1} \int_{t_{\max}-4\pi/\omega}^{t_{\max}} E(t)dt, \tag{A3}$$

$$\langle E_0\rangle \equiv (4\pi/\omega)^{-1} \int_{t_0}^{t_0+4\pi/\omega} E(t)dt, \tag{A4}$$

in the $\alpha-\tau$ parameter plane for a ring of $N = 5$ oscillators with $t_0 = 40, t_{\max} = 400$, and where the retardation term and the exact AR force are solely applied to a single oscillator (u_3). The dashed line indicates the critical damping $\eta = \eta_c$ [cf. Eq. (16)] separating the amplification regime from the extinction (regularization) regime (blank region). The chains present a chaotic attractor for $\alpha = F_n(t) = 0$. Points A, B, C y D are representative of the different regions in the $\alpha-\tau$ parameter plane. The time series of oscillators position and ring energy corresponding to such points and different values of the coupling λ and the amplitude γ of the homogeneous periodic driving are shown in Figs. 7-10. One sees different regularized behaviors depending on whether or not the homogeneous harmonic force acts on the ring (compare Figs. 7 and 9 with Figs. 8 and 10, respectively). Additionally, synchronization of the regularized solutions of the full ring is achieved for sufficiently large values of the coupling, while in the weak coupling regime desynchronization appears by groups of oscillators (compare Figs. 7 and 8 with Figs. 9 and 10, respectively).

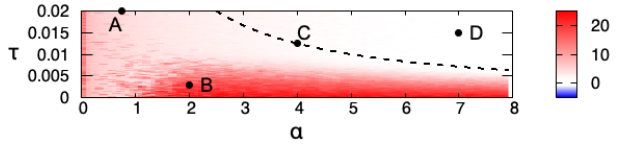

FIG. 6: Average energy amplification, $\log\left[\langle E\rangle / \langle E_0\rangle\right]$ [cf. Eqs. (A3) and (A4)], in the $\alpha-\tau$ parameter plane for $\beta = 1, \eta = 0.05, \gamma = 0.1, \omega = 0.21, \lambda = 0.05, N = 5$ with $t_0 = 40, t_{\max} = 400$. Points A, B, C, D correspond to the values $(\alpha, \tau) = (0.75, 0.02), (2, 0.003), (4, 0.0125), (7, 0.015)$, respectively.

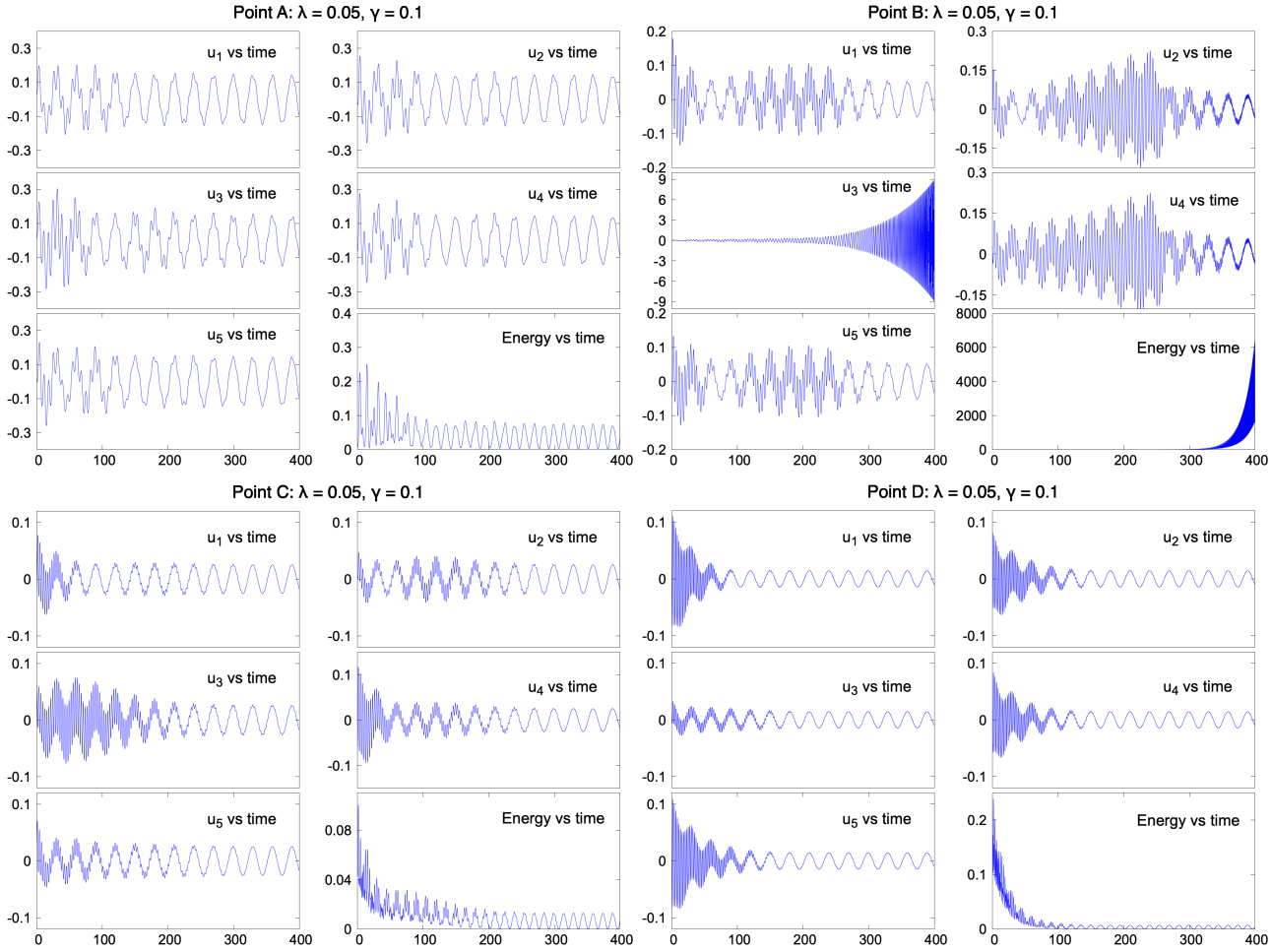

FIG. 7: Time series of oscillators position and ring energy for $\lambda = 0.05, \gamma = 0.1$ and the values of (α, τ) corresponding to the points A, B, C, D shown in Fig. 6. Fixed parameters: $N = 5, \beta = 1, \eta = 0.05$, $\omega = 0.21$.

[1] E. M. McMillan, Phys. Rev. **68**, 144 (1945).
[2] D. Bohm and L. Foldy, Phys. Rev. **70**, 249 (1946).
[3] W. K. Liu, B. Wu, and J. M. Yuan, Phys. Rev. Lett. **75**, 1292 (1995).
[4] R. Malhotra, Nature **365**, 819 (1993).
[5] J. Fajans and L. Friedland, Am. J. Phys. **69**, 1096 (2001).
[6] G. Klughertz, P.-A. Hervieux, and G. Manfredi, J. Phys. D: Appl. Phys. **47**, 345004 (2014).
[7] A. Kovaleva, Phys. Rev. E **98**, 052227 (2018), and references therein.
[8] K. Gomberoff, H. Higaki, C. Kaga, K. Ito, and H. Okamoto, Phys. Rev. E **94**, 043204 (2016).
[9] D. Cyncynates, T. Giurgica-Tiron, O. Simon, and J. O. Thompson, Phys. Rev. D **105**, 055005 (2022).
[10] D. Goswami, Phys. Rep. **374**, 385 (2003).
[11] R. Chacón, Europhys. Lett. **70**, 56 (2005).
[12] R. Chacón, Phys. Rev. E **78**, 066608 (2008).
[13] R. Chacón, J. Phys. A: Math. Theor. **43**, 222002 (2010).
[14] A. Kovaleva, Philos. Trans. R. Soc. A **375**, 20160213 (2017).
[15] For a recent review, see H. Wernecke, B. Sándor, and C. Gros, Phys. Rep. **824**, 1 (2019), and references therein.
[16] This comes ultimately from the fact that $4K(m)$ is the real period of cn.
[17] F. Cariello and M. Tabor, in *Painlevé Transcendents*, edited by D. Levi and P. Winternitz (Plenum, New York, 1992).
[18] H. Goldstein, *Classical Mechanics* (Addison-Wesley, Reading, 1980).

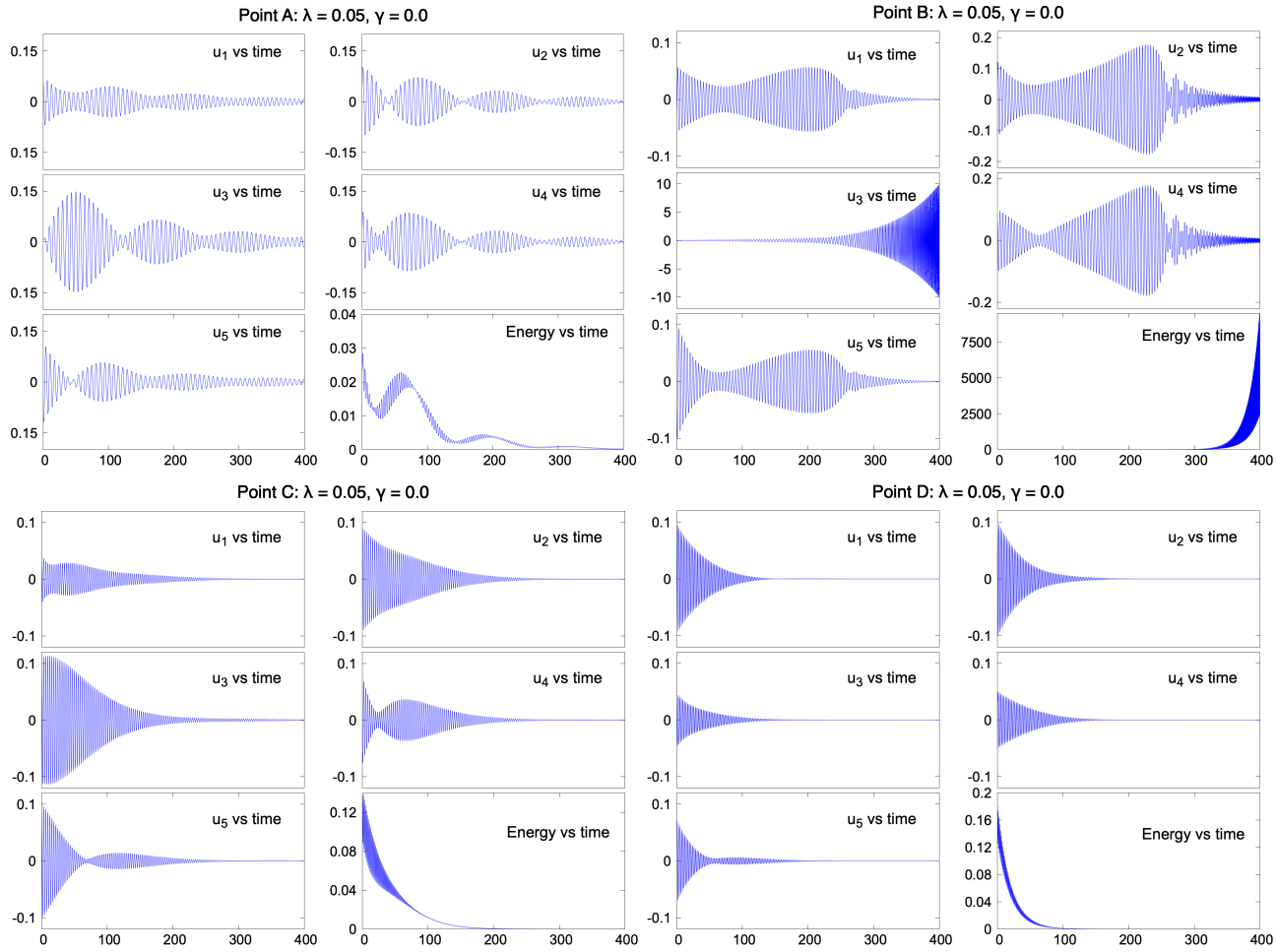

FIG. 8: Time series of oscillators position and ring energy for $\lambda = 0.05, \gamma = 0$ and the values of (α, τ) corresponding to the points A, B, C, D shown in Fig. 6. Fixed parameters: $N = 5, \beta = 1, \eta = 0.05$, $\omega = 0.21$.

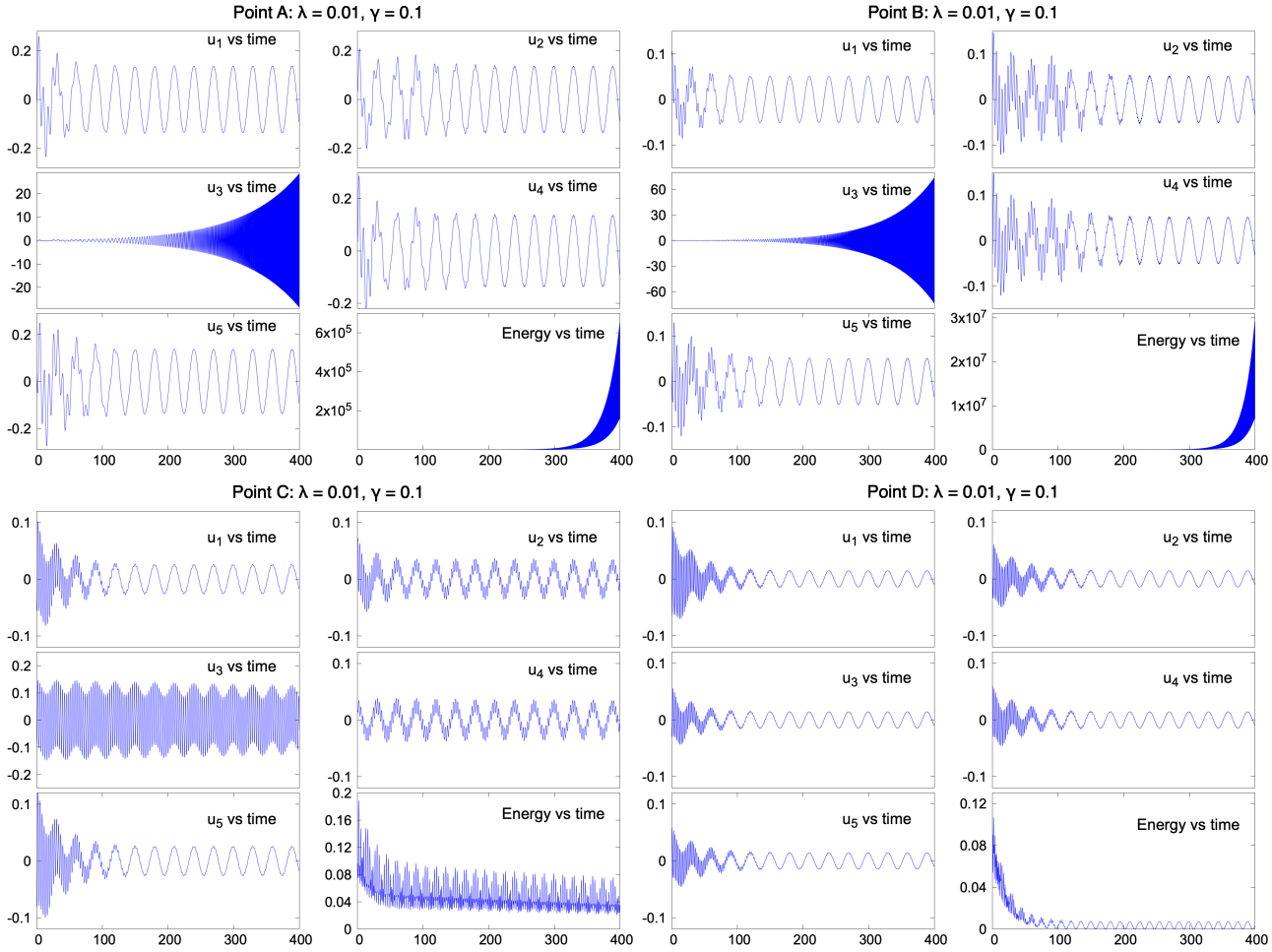

FIG. 9: Time series of oscillators position and ring energy for $\lambda = 0.01, \gamma = 0.1$ and the values of (α, τ) corresponding to the points A, B, C, D shown in Fig. 6. Fixed parameters: $N = 5, \beta = 1, \eta = 0.05$, $\omega = 0.21$.

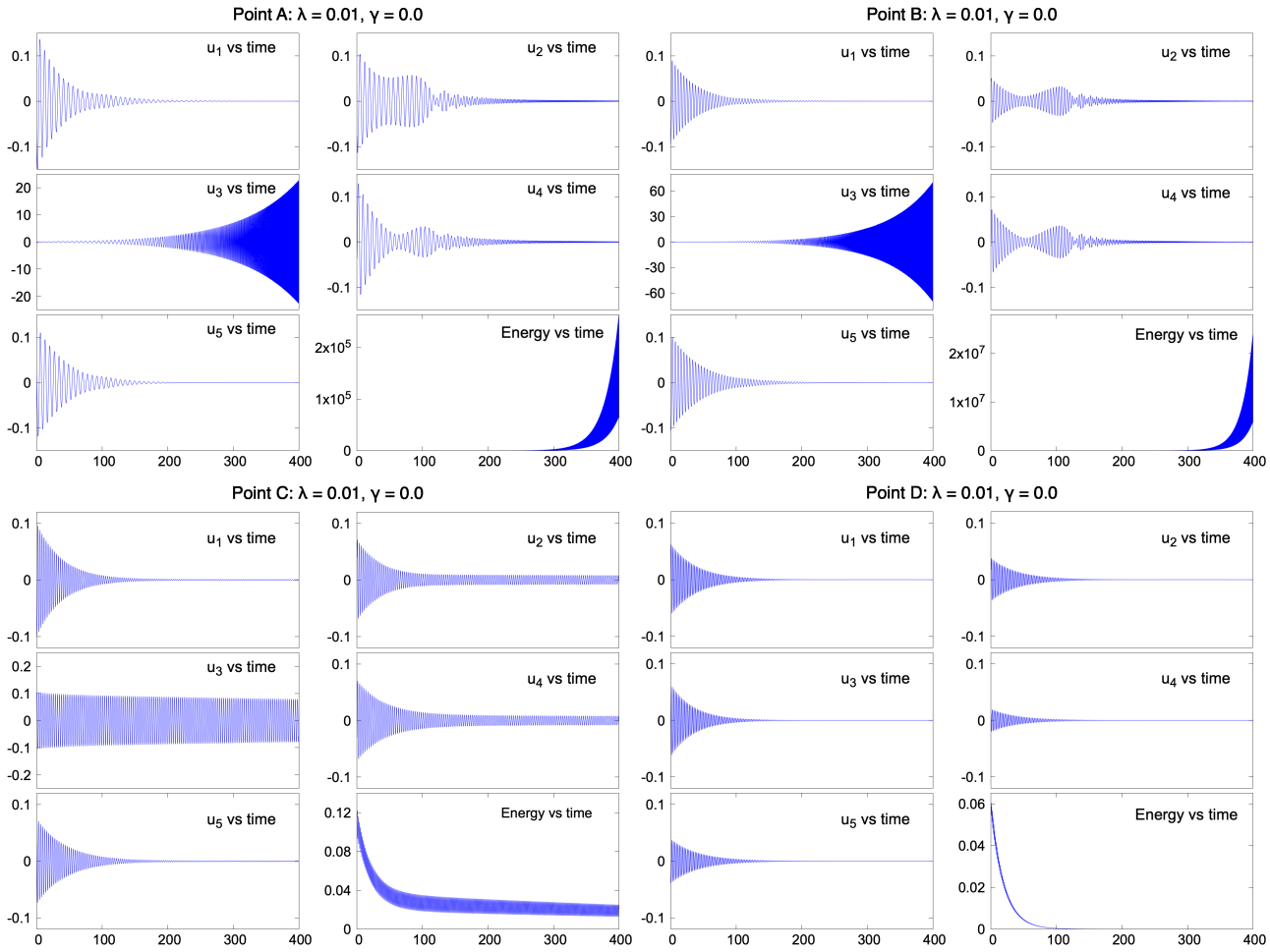

FIG. 10: Time series of oscillators position and ring energy for $\lambda = 0.01, \gamma = 0$ and the values of (α, τ) corresponding to the points A, B, C, D shown in Fig. 6. Fixed parameters: $N = 5, \beta = 1, \eta = 0.05$, $\omega = 0.21$.